Publ. Astron. Obs. Belgrade No. 86 (2009), 83 - 88 *Contributed paper*

TRIGGERED STAR FORMATION IN NEARBY HIGH GALACTIC LATITUDE CLOUDS: PRELIMINARY OVERVIEW

N. MARTINOVIĆ[1], S. NIKOLIĆ[2,4], M. KUN[3], D. MARDONES[4] and J. EISLÖFFEL[5]

[1] *Department of Astronomy, Faculty of Mathematics, Studentski trg 16, 11000 Belgrade, Serbia*
E–mail: nem_mart@yahoo.com

[2] *Astronomical Observatory, Volgina 7, 11060 Belgrade 38, Serbia*

[3] *Konkoly observatory, Konkoly Thege Miklós út 15-17, H-1121 Budapest, Hungary*

[4] *Department of Astronomy, University of Chile, Casilla 36-D, Santiago, Chile*

[5] *Thüringer Landessternwarte Tautenburg, Sternwarte 5, 007778 Tautenburg, Germany*

Abstract. The importance of triggered star formation is a current matter of debate. In this paper we approach the issue by doing small-scale, deep-field study of low-mass star formation in Orion. Using the VLT/ISAAC we performed pointed observation in Js, H and K bands towards cometary-shaped, high Galactic latitude molecular clouds, which are dynamically influenced by the Orion-Eridanus bubble. We present preliminary photometry results and YSOs classification of one targeted region, the LBN917 molecular cloud. Tentative result suggests an existence of a preferred direction of the star formation wave propagation in the region.

1. INTRODUCTION

Traditionally star formation is thought to appear in two modes. In a so-called isolated mode number of newly formed stars is at most $N = 1$ or 2, and the formation alone is a consequence of gravitation collapse within a molecular cloud. On the other side in a clustered mode number of young stars is $N >> 1$ and there is a strong influence of the neighboring stars. Regarding stellar masses, the first mode forms exclusively low-mass stars, while result of the latter mode is a mixture of low, intermediate and high mass stars. What fraction of stars in the Galaxy are born in each mode is a matter of debate. Several authors have suggested that the majority of stars form in clusters (e.g. Evans 1999). Based on the known Galactic open clusters data and including some theoretical considerations of the star formation process, Adams and Myers (2001) have proposed finer divisions in the modes of star formation process with at least three principal modes: (1) isolated singles and binaries, (2) groups and (3) clusters. They suggest that the group mode may be dominant, while at the same time the birth of those stars is less influenced by their environment. Furthermore, numerical studies of Hennebelle et al. (2004) have shown that external compression on cloud cores favors the fragmentation leading to formation of stellar groups.

The very onset of star formation in individual molecular cores, i.e., in the case of isolated mode, seems to be strongly correlated with the presence of external pressure from stars in the vicinity (e.g. Elmegreen 2002). This suggests that even for the isolated star formation mode an existence of an outer trigger could be relevant, thus a triggered star formation may be far more important than previously assumed. So far, molecular clouds where there is evidence of an externally initiated star formation process lie at the surfaces of old supernovas bubbles or nearby large associations of young OB stars. An example where a low mass star formation was possibly triggered by a few million years old SN explosion is L1251 dark cloud in the Cepheus Flare region (e.g. Kun and Prusti 1993 and Nikolić et al. 2003). Another example of a triggered onset of star formation may be the Orion-Eridanus Bubble (Brown et al. 1995). This superbubble was formed by stellar winds and supernova explosions of massive stars in the Orion OB1 association in the last ten million years. Indications that the bubble might have triggered star formation in the region are found in the dark cloud L1616 (e.g. Alcalá et al. 2004, Stanke et al. 2002) and L1622 (Kun et al. 2008).

Further suggested example is the IC2118 cloud complex. IC2118 is a long, filamentary reflection nebula illuminated by Rigel, located at 210 pc from the Sun (Kun et al. 2001), which lies on the front side of the Orion-Eridanus Bubble. The ages of the pre-main sequence stars found in the complex (Kun et al. 2004) are compatible with the assumption that star formation has been triggered by the superbubble. This work is an attempt to assess the influence of the OB1 association on its larger-scale environment and to find signatures of a propagation wave of star formation. More specifically, we aim to confirm that triggered star formation in the IC2118 region and induced by the Ori OB1 association is currently progressing in a S, S-E direction with respect to the association.

2. OBSERVATION AND DATA REDUCTION

2. 1. OBSERVATIONS

We targeted several dark clouds (NGC1788-South, Lynd's Bright Nebula, LBN 917) and areas of new pre-main sequence (PMS) stars and young stellar objects (YSO) in dark cloud IC2118 (Kun et al. 2004). Near-infrared (NIR) Js, H, Ks, L and M imaging was conducted using ESO Antu (VLT Unit 1) telescope equipped with the short-wavelength (Hawaii Rockwell, $1-2.5\mu m$) and long- wavelength arm (InSb Alladin, $3-5\mu m$) of the ISAAC instrument. The ISAAC camera (Moorwood et al. 1998) contains a 1024 x 1024 pixel near- infrared array and fields of view that are 2.5' x 2.5' and 1.25' x 1.25' on the sky for the SW and LW detectors, respectively. At the distance of IC2118 they cover areas of 0.15 x 0.15 and 0.075 x 0.075 parsecs, respectively. The observations were performed in service mode in several sessions in 2004, 2005 and 2006. Exposure times were 2 to 12s. Estimated limiting magnitudes at detection limit, $S/N = 3$, are: $J_S = 22.0^m$, $H = 21.6^m$ and $K_S = 21.3^m$, with lowest expected luminosity of: $L_{J_S} = 3.4 \cdot 10^{-4} L_\odot$, $L_K = 5.0 \cdot 10^{-4} L_\odot$ and $L_{K_S} = 6.5 \cdot 10^{-4} L_\odot$.

2. 2. DATA REDUCTION

The received reduced data using the ISAAC's pipeline process were verified by election of several random raw images that were reduced manually using the IRAF reduction software routines[1]. With respect to the data reduction there are several limitations of the ISAAC instrument. There is no bias frame (no zero exposures frames) and only twilight flats are available, with no dome flats. We adopted the following routine in data reduction: raw images were dark subtracted and flat fielded with a median of dusk and dawn twilight flats using IRAF tasks from the NOAO package. Brief analysis of the resulted images shows that there is a large scale gradient across the image which has ∼ 2% amplitude. Illumination correction is calculated from the object frames using MKSKYCOR task from the NOAO package. Next came bad pixels and cosmic rays image cleaning. Unfortunately because of the absence of the bias frames there are significant residuals around the middle of the frames in form of small, but nevertheless noticeable, jumps in the vertical direction. To remove this excess noise (the 'jump') we averaged the image along rows and subtracted the resulting one dimensional image from each column of the original image. For this we used the FLAT1D task. The sky subtraction had to be calculated from object frames using the recommended XDIMSUM package. The final result i.e., the reduced images were compared to the images reduced by the ISAAC pipeline process. No significant differences were found, and for further analysis the pipelined data were used.

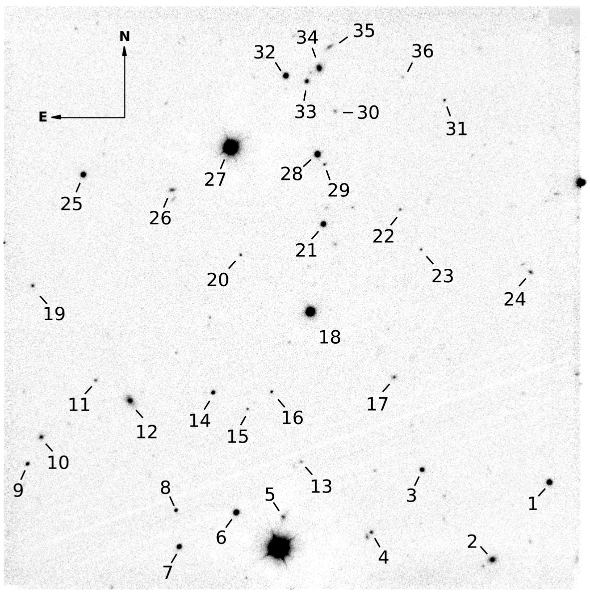

Figure 1: The JHK three-color composite of LBN917's observed field of view. Colors are intentionally inverted for easier source indentification and stars are labeled for easier cross-corelation with Table 1.

[1]IRAF is distributed by the National Optical Astronomy Observatories, which are operated by the Association of Universities for Research in Astronomy, Inc., under cooperative agreement with the National Science Foundation.

3. PRELIMINARY RESULTS

We chose the LBN917 cloud for presenting preliminary results and analysis. Fig. 1 shows the three-color composite of the observed field of view of LBN917 cloud (after data reduction), where standard color classification is used (J_S - blue, H - green, K_S - red). Columns 2, 4 and 6 in Table 1 give the preliminary photometry, columns 3, 5 and 7 - the estimated photometry errors. Finally, the derived colors are shown in columns 8 and 10. Photometry of an object was performed as described in the previous section. Using the APPHOT package and the QPHOT task, instrumental magnitudes for selected stars within field of view were calculated. A typical radial aperture of 4-5 times the FWHM was adopted. These instrumental magnitudes were transformed into standard magnitudes using the ESO provided standard stars images and their comparison with the 2MASS catalog values. The atmospheric extinction correction was performed using the Paranal Observatory tables for the atmospheric IR extinction.

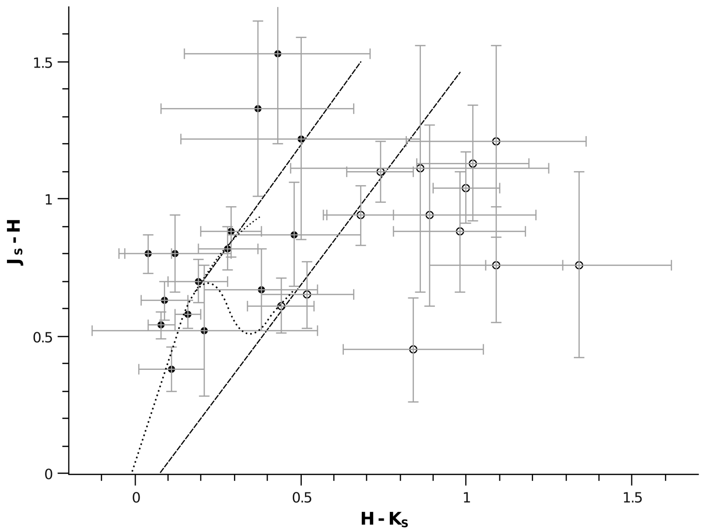

Figure 2: The JHK color-color diagram for LBN917. The two dashed lines on the graph form the reddening band for normal stellar atmospheres. The objects with colors that fall outside and right of this band are the sources with intrinsic infrared excess emission. The curves show the colors for main-sequence stars (lower branch) and giants (upper branch). Open circles represent possible YSO candidates.

Fig. 2 shows the $J_S - H$ vs. $H - K_S$ color-color diagram of the detected objects in LBN917. The stars in the field of view populate the area of older YSOs, and are tentatively classified as a Class II YSOs and Class III YSOs i.e., as classic T Tau stars and weak-line T Tau stars, respectively.

Significant blooming is visible around large unmarked star in the bottom of the field of view in Fig. 1 indicates a possible image saturation. Further analysis of star's FWHM profile confirmed saturation, excluding the star from the analysis.

Table 1: The JHK standard magnitudes along with $(J_S - H)$ and $(H - K_S)$ for LBN917 molecular cloud. YSO candidates are bolded, and italic entries are excluded from the graph due to the large errors.

No.	J_S	ΔJ_S	H	ΔH	K_S	ΔK_S	$J_S - H$	Δ_{J_S-H}	$H - K_S$	Δ_{H-K_S}
1	17.46	0.05	16.58	0.04	16.28	0.04	0.88	0.09	0.29	0.09
2	**18.50**	**0.07**	**17.46**	**0.06**	**16.45**	**0.04**	**1.04**	**0.13**	**1.00**	**0.10**
3	**18.42**	**0.06**	**17.77**	**0.06**	**17.24**	**0.07**	**0.65**	**0.12**	**0.52**	**0.14**
4	**19.46**	**0.11**	**18.33**	**0.10**	**17.30**	**0.07**	**1.13**	**0.21**	**1.02**	**0.17**
5	**19.72**	**0.16**	**18.78**	**0.17**	**17.88**	**0.14**	**0.94**	**0.33**	**0.89**	**0.32**
6	17.15	0.04	16.35	0.03	16.30	0.04	0.80	0.07	0.04	0.07
7	**17.84**	**0.05**	**17.23**	**0.05**	**16.78**	**0.05**	**0.61**	**0.10**	**0.44**	**0.10**
8	**19.02**	**0.08**	**18.57**	**0.11**	**17.72**	**0.10**	**0.45**	**0.19**	**0.84**	**0.21**
9	19.24	0.10	18.72	0.14	18.50	0.20	0.52	0.24	0.21	0.34
10	**19.40**	**0.11**	**18.52**	**0.11**	**17.53**	**0.08**	**0.88**	**0.22**	**0.98**	**0.20**
11	*20.77*	*0.30*	*19.75*	*0.30*	*18.35*	*0.15*	*1.02*	*0.60*	*1.39*	*0.46*
12	**18.39**	**0.06**	**17.29**	**0.05**	**16.54**	**0.05**	**1.10**	**0.11**	**0.74**	**0.10**
13	20.29	0.20	19.07	0.17	18.56	0.19	1.22	0.37	0.50	0.36
14	18.67	0.07	18.00	0.08	17.61	0.09	0.67	0.15	0.38	0.17
15	*20.90*	*0.33*	*19.39*	*0.22*	*19.21*	*0.30*	*1.51*	*0.55*	*0.17*	*0.53*
16	*19.98*	*0.16*	*19.21*	*0.19*	*19.30*	*0.33*	*0.77*	*0.35*	*-0.10*	*0.53*
17	**19.93**	**0.16**	**19.17**	**0.18**	**17.82**	**0.10**	**0.76**	**0.34**	**1.34**	**0.28**
18	14.94	0.03	14.36	0.02	14.19	0.02	0.58	0.05	0.16	0.04
19	20.20	0.20	18.67	0.13	18.23	0.15	1.53	0.33	0.43	0.28
20	*20.45*	*0.23*	*19.76*	*0.30*	*19.85*	*0.51*	*0.69*	*0.53*	*-0.10*	*0.81*
21	17.55	0.04	16.73	0.04	16.44	0.04	0.82	0.08	0.28	0.09
22	*20.65*	*0.27*	*20.21*	*0.44*	*19.05*	*0.26*	*0.44*	*0.71*	*1.15*	*0.70*
23	*21.71*	*0.65*	*21.52*	*1.39*	*19.61*	*0.42*	*0.19*	*2.04*	*1.90*	*1.81*
24	**20.08**	**0.18**	**18.87**	**0.17**	**17.77**	**0.09**	**1.21**	**0.35**	**1.09**	**0.27**
25	17.19	0.04	16.81	0.04	16.69	0.05	0.38	0.08	0.11	0.10
26	**19.34**	**0.10**	**18.58**	**0.11**	**17.48**	**0.08**	**0.76**	**0.21**	**1.09**	**0.20**
27	13.13	0.03	12.59	0.02	12.50	0.02	0.54	0.05	0.08	0.04
28	16.81	0.04	16.18	0.03	16.08	0.04	0.63	0.07	0.09	0.07
29	18.69	0.07	17.89	0.07	17.76	0.09	0.80	0.14	0.12	0.17
30	**20.49**	**0.24**	**19.38**	**0.21**	**18.51**	**0.17**	**1.11**	**0.45**	**0.86**	**0.39**
31	*20.02*	*0.17*	*20.78*	*0.74*	*19.51*	*0.39*	*-0.76*	*0.91*	*1.26*	*1.14*
32	17.31	0.04	16.61	0.04	16.41	0.04	0.70	0.08	0.19	0.09
33	19.09	0.09	18.22	0.10	17.73	0.10	0.87	0.19	0.48	0.20
34	**18.25**	**0.06**	**17.31**	**0.05**	**16.62**	**0.05**	**0.94**	**0.11**	**0.68**	**0.10**
35	19.99	0.18	18.66	0.14	18.28	0.15	1.33	0.32	0.37	0.29
36	*23.18*	*2.52*	*19.99*	*0.37*	*21.55*	*2.47*	*3.19*	*2.89*	*-1.57*	*2.85*

The distance and thus the exact position with respect to the Ori-Eri center of LBN917 is not known. Based on a large-scale ^{12}CO and ^{13}CO mapping of the whole Orion region and the observed central velocities $V_{LSR} = -6$ to -4 km/s, Bally at el. (1991) estimated that the cloud is at the distance of 500pc. Such a distance would place LBN917 deep within the Orion-Eridanus Bubble. If this relative geometry is correct, in LBN917 we could expect to find YSO candidates that are older compared to YSO candidate stars in molecular clouds located closer towards the surface of the Ori-Eri Bubble. The preliminary classification of the objects in the LBN917 field of view seems to indicate existence of a preffered direction of the wave propagation of star formation in this area with respect to the center of Ori-Eri Bubble, implying that in the Orion region a triggered star formation might be significant.

More thorough analysis of this presented result like e.g., investigating physical association of the detected objects with the LBN917 molecular cloud, excluding any foreground and background stars that might contaminate data and performing spectroscopy of YSO candidates could confirm this preliminary results.

Acknowledgments

Financial support from the Serbian Ministry of Science and Technological Development grant No. 146016 (S.N.), the Hungarian OTKA grant T049082 (M.K.), the Chilean Centro de Astrofisica FONDAP No. 15010003 (S.N. and D.M.) and the Deutsches Zentrum für Luft- und Raumfahrt under grant 50 OR 0009 (J.E.) is acknowledged.

References

Adams, Fred C., Myers, Philip, C.: 2001, *Astrophys. J.*, **553**, Issue 2, 744.

Alcalá, J. M., Wachter, S., Covino, E., Sterzik, M. F., Durisen, R. H., Freyberg, M. J., Hoard, D. W., Cooksey, K.: 2004, *Astron. Astrophys.*, **416**, 677.

Bally, J., Langer, W. D., Wilson, R. W., Stark, A. A., Pound, M. W.: 1991, Fragmentation of Molecular Clouds and Star Formation: Proceedings of the 147th Symposium of the IAU, 11.

Brown, A. G. A., Hartmann, D., Burton, W. B.: 1995, *Astron. Astrophys.*, **300**, 903.

Elmegreen, Bruce G.: 2002, *Astrophys. J.*, **577**, Issue 1, 206.

Evans, Neal J., II: 1999, *Annu. Rev. Astron. Astrophys.*, **37**, 311.

Hennebelle, P., Whitworth, A. P., Cha, S.-H., Goodwin, S. P.: 2004, *Mon. Not. R. Astron. Soc.*, **348**, Issue 2, 687.

Kun, M., Prusti, T.: 1993, *Astron. Astrophys.*, **272**, 235.

Kun, Maria, Aoyama, Hiroko, Yoshikawa, Nao, Kawamura, Akiko, Yonekura, Yoshinori, Onishi, Toshikazu, Fukui, Yasuo: 2001, *Publ. Astron. Soc. Japan*, **53**, 1063.

Kun, M., Prusti, T., Nikolić, S., Johansson, L. E. B., Walton, N. A.: 2004, *Astron. Astrophys.*, **418**, 89.

Kun, M., Balog, Z., Mizuno, N., Kawamura, A., Gáspár, A., Kenyon, S. J., Fukui, Y.: 2008, *Mon. Not. R. Astron. Soc.*, **Online Early**.

Lada, Charles J., Adams, Fred C.: 1992, *Astrophys. J.*, **393**, 278.

Moorwood, A., Cuby, J.-G. and 19 more authors: 1998, *Messenger*, **94**, 7.

Nikolić, S., Johansson, L. E. B., Harju, J.: 2003, *Astron. Astrophys.*, **409**, 941.

Stanke, T., Smith, M. D., Gredel, R., Szokoly, G.: 2002, *Astron. Astrophys.*, **393**, 251.